

Efficient TLM-Based Approach for Compact Modeling of Anisotropic Materials and Composites

Miloš D. Kostić¹, Nebojša S. Dončov², Zoran Ž. Stanković², and John D. Paul³

¹Innovation Center of Advanced Technologies, Niš, 18000, Serbia
r.i.p.romeo@gmail.com

²Faculty of Electronic Engineering
University of Niš, Niš, 18000, Serbia
nebojsa.doncov@elfak.ni.ac.rs, zoran.stankovic@elfak.ni.ac.rs

³Electromagnetics scientist, Nottingham, NG1, United Kingdom
john.derek.paul@gmail.com

Abstract — Compact modeling approach of anisotropic media by using the Z-TLM method is proposed. Thin anisotropic multilayer material is efficiently described through connection procedure between two Z-TLM mesh cells, by using the scattering parameters to create a digital filter-based compact model. Model is incorporated into non-uniform TLM grid given here in a form fully complying with the originally proposed Z-TLM method algorithm. Accuracy and efficiency of the compact model is confirmed on a few examples through comparison with the fine mesh results.

Index Terms — Anisotropic materials and composites, compact model, non-uniform grid, Z-TLM method.

I. INTRODUCTION

Discrete time modeling techniques have been used by researchers for years to simulate and observe propagation and distribution of electromagnetic (EM) fields inside of different media. The two most popular modeling techniques based on time and space discretization are the Finite Difference Time Domain (FDTD) method [1] and the Transmission Line Matrix (TLM) method [2]. Generally, the FDTD method is often the favored numerical technique for solving different kinds of EM problems ranging from antenna problems, electromagnetic compatibility, microwave systems, etc. However, the TLM method, since it was established in 1970 by P. B. Johns, has proven to have certain advantages in modeling of specific complex structures and nonlinear materials.

TLM algorithm is highly localized since electric and magnetic fields are solved in the center of the TLM cell at the same time. In addition to that, the fact that any change in the state of a TLM cell affects only its immediate neighbors at the next computational step

makes it more suited for modeling of anisotropic and bianisotropic media. EM fields on cell boundaries can be determined without necessity to perform temporal interpolation and field averaging, which is another important feature. An enhancement of the TLM method with Z-transform techniques (so-called Z-TLM method) [3] enables a direct mapping of dispersive EM material properties into the time-domain in order to study their time-harmonic and transient response. The Z-TLM method has already been used for simulation of linear isotropic and anisotropic media, bi-isotropic and quantum materials as well as materials with nonlinear and metamaterial properties [3-9].

In order to properly simulate behavior of geometrically small but electrically important features in an otherwise large modeling space, by using traditional approach in discrete time modeling methods, an extremely fine mesh is required. With intention to overcome this computationally and time costly requirement, and thus improve efficiency, development of compact models is required. Compact models allow for using coarser mesh, e.g. reducing all thin material cells to single boundary condition based on material panel scattering parameters [10] (sort of “black box” approach where only input and output values are observed) or by using retrieval methods for effective EM parameter extraction from the scattering parameters of thin material in order to model it and observe EM field behavior within its interior boundaries [11].

Material can be defined as anisotropic when values of one or more EM properties (such as conductivity, permittivity and permeability) depend on direction of EM propagation e.g., when EM properties are functions of the coordinate system orientation. Micro-structure of anisotropic materials consists out of different layers created and connected naturally (wood, different crystals,

minerals and rocks, etc.) or intentionally in structural/man-made (reinforced, ribbed, perforated, layered materials etc.). General anisotropic materials, besides coefficients on main diagonal (a_{xx} , a_{yy} , a_{zz}) in EM property matrix, contain additional coefficients which describe codependency based on direction (a_{xy} , a_{xz} , a_{yx} , ...). This makes modeling of materials like carbon, graphite, glass and other composites more challenging.

In this paper, the discretization of Maxwell's equations and constitutive relations for simulation of general anisotropic and dispersive materials, using the Z-TLM method in non-linear grid, is described. The ways to describe the TLM method for modeling of dispersive and anisotropic media and/or using non-uniform meshes have been given in [12, 13] but here is given in a form that fully complies with the Z-TLM method initially proposed in [3-5]. In addition to that, an efficient approach for compact modeling of composite anisotropic materials, previously applied on a one-dimensional case [14], is here given in a generalized form and later used in a two-dimensional (2-D) problem. It uses the scattering parameters of a composite structure consisting in general of n material layers, obtained from e.g., fine Z-TLM mesh, to create a digital filter-based compact model where composite structure is efficiently described with boundary condition between two Z-TLM mesh cells. Compared to other network-based methods such as ladder type method [15], the proposed approach is more general and the created model is more easily and more memory efficiently incorporated into the TLM connection procedure. Accuracy and efficiency of the approach is confirmed on a few examples through comparison with the fine Z-TLM mesh results.

II. DISCRETIZATION OF MAXWELL'S EQUATIONS FOR NON-UNIFORM MESH

For non-uniform TLM cell, where one or more directional space steps (Δx , Δy , and Δz) are not equal, a compact form of Maxwell's curl equations is established through constitutive relations for electric and magnetic current and flux densities:

$$\begin{bmatrix} \nabla \times \underline{H} \\ -\nabla \times \underline{E} \end{bmatrix} - \begin{bmatrix} \underline{J}_{ef} \\ \underline{J}_{mf} \end{bmatrix} = \frac{\partial}{\partial t} \begin{bmatrix} \epsilon_0 \underline{E} \\ \mu_0 \underline{H} \end{bmatrix} + \begin{bmatrix} \underline{\sigma}_e * \underline{E} \\ \underline{\sigma}_m * \underline{H} \end{bmatrix} + \frac{\partial}{\partial t} \begin{bmatrix} \epsilon_0 \underline{\chi}_e & \underline{\xi}_r / c \\ \underline{\zeta}_r / c & \mu_0 \underline{\chi}_m \end{bmatrix} * \begin{bmatrix} \underline{E} \\ \underline{H} \end{bmatrix}, \quad (1)$$

where $*$ denotes time domain convolution, \underline{J}_{ef} , \underline{J}_{mf} represent electric and magnetic current densities vectors, $\underline{\sigma}_e$, $\underline{\sigma}_m$ and $\underline{\chi}_e$, $\underline{\chi}_m$ are electric and magnetic conductivity and susceptibility matrices respectively, ϵ_0 , μ_0 are free space permittivity and permeability, and $\underline{\xi}_r$, $\underline{\zeta}_r$ are dimensionless matrices describing magnetoelectric coupling.

By expanding curl terms of (1) in Cartesian coordinates and introducing a compact notation with defined matrices and vectors, the following expression is

formed:

$$-\begin{bmatrix} \nabla \times \underline{H} \\ -\nabla \times \underline{E} \end{bmatrix} = \begin{bmatrix} \frac{1}{\eta_0} \underline{A}^{-1} & \underline{0} \\ \underline{0} & \underline{A}^{-1} \end{bmatrix} \cdot \begin{bmatrix} \underline{0} & \underline{C} \\ -\underline{C} & \underline{0} \end{bmatrix} \cdot \begin{bmatrix} \underline{V} \\ \underline{i} \end{bmatrix}. \quad (2)$$

In (2) η_0 is intrinsic impedance of free-space, \underline{V} and \underline{i} are vectors of voltages and currents defined in the center of TLM cell while the matrix of inverse cell areas and normalized curl matrix are represented as:

$$\underline{A}^{-1} = \begin{bmatrix} (\Delta z \Delta y)^{-1} & 0 & 0 \\ 0 & (\Delta z \Delta x)^{-1} & 0 \\ 0 & 0 & (\Delta y \Delta x)^{-1} \end{bmatrix}, \underline{C} = \begin{bmatrix} 0 & -\partial_z & \partial_y \\ \partial_z & 0 & -\partial_x \\ -\partial_y & \partial_x & 0 \end{bmatrix}, \quad (3)$$

where ∂_x , ∂_y , ∂_z are normalized spatial derivatives in x , y and z direction respectively.

After applying the field circuit equivalences and defining free-current vectors, free current density terms are formed as:

$$-\begin{bmatrix} \underline{J}_{ef} \\ \underline{J}_{mf} \end{bmatrix} = \begin{bmatrix} \frac{1}{\eta_0} \underline{A}^{-1} & \underline{0} \\ \underline{0} & \underline{A}^{-1} \end{bmatrix} \cdot \begin{bmatrix} \underline{i}_{ef} \\ \underline{V}_{mf} \end{bmatrix}. \quad (4)$$

Vector matrix form of time derivative field term is established by transforming time derivative operator $\frac{\partial}{\partial t}$:

$$-\frac{\partial}{\partial t} \begin{bmatrix} \epsilon_0 \underline{E} \\ \mu_0 \underline{H} \end{bmatrix} = \left(\frac{2\alpha_t}{\Delta \ell} \right) \frac{\partial}{\partial T} \begin{bmatrix} \frac{1}{\eta_0} \underline{\Delta}^{-1} & \underline{0} \\ \underline{0} & \underline{\Delta}^{-1} \end{bmatrix} \cdot \begin{bmatrix} \underline{V} \\ \underline{i} \end{bmatrix}, \quad (5)$$

by defining the matrix of inverse cell length $\underline{\Delta}^{-1}$ as:

$$\underline{\Delta}^{-1} = \begin{bmatrix} \Delta x^{-1} & 0 & 0 \\ 0 & \Delta y^{-1} & 0 \\ 0 & 0 & \Delta z^{-1} \end{bmatrix}, \quad (6)$$

and introducing parameter α_t as the time-step adjustment factor so that:

$$\frac{\partial}{\partial t} = \frac{1}{\Delta t} \frac{\partial}{\partial T} = \frac{2c\alpha_t}{\Delta \ell} \frac{\partial}{\partial T}. \quad (7)$$

Compact notation of electric and magnetic conductivity terms is defined in order to represent them as:

$$-\begin{bmatrix} \underline{\sigma}_e * \underline{E} \\ \underline{\sigma}_m * \underline{H} \end{bmatrix} = \begin{bmatrix} \frac{1}{\eta_0} \underline{A}^{-1} & \underline{0} \\ \underline{0} & \underline{A}^{-1} \end{bmatrix} \cdot \begin{bmatrix} \underline{g}_e * \underline{V} \\ \underline{r}_m * \underline{i} \end{bmatrix}. \quad (8)$$

Time derivative susceptibility term in normalized form yields:

$$-\frac{\partial}{\partial t} \begin{bmatrix} \epsilon_0 \underline{\chi}_e & \underline{\xi}_r / c \\ \underline{\zeta}_r / c & \mu_0 \underline{\chi}_m \end{bmatrix} * \begin{bmatrix} \underline{E} \\ \underline{H} \end{bmatrix} = \left(\frac{2\alpha_t}{\Delta \ell} \right) \frac{\partial}{\partial T} \begin{bmatrix} \underline{\chi}_e / \eta_0 & \underline{\xi}_r / \eta_0 \\ \underline{\zeta}_r & \underline{\chi}_m \end{bmatrix} \cdot \begin{bmatrix} \underline{\Delta}^{-1} & \underline{0} \\ \underline{0} & \underline{\Delta}^{-1} \end{bmatrix} * \begin{bmatrix} \underline{V} \\ \underline{i} \end{bmatrix}. \quad (9)$$

Using expressions above along with defining background susceptibilities matrix,

$$\underline{\underline{\chi}}_b = \left(\frac{2\alpha_t}{\Delta\ell} \right) \underline{\underline{A}} \underline{\underline{\Delta}}^{-1} - \underline{\underline{1}}, \quad (10)$$

where $\underline{\underline{1}}$ is identity matrix, a normalized form of Maxwell's equations is assembled as:

$$\begin{bmatrix} 0 & \underline{\underline{C}} \\ -\underline{\underline{C}} & 0 \end{bmatrix} \cdot \begin{bmatrix} \underline{\underline{V}} \\ \underline{\underline{i}} \end{bmatrix} - \begin{bmatrix} \underline{\underline{i}}_{ef} \\ \underline{\underline{V}}_{mf} \end{bmatrix} = 2 \frac{\partial}{\partial T} \begin{bmatrix} \underline{\underline{V}} \\ \underline{\underline{i}} \end{bmatrix} + 2 \frac{\partial}{\partial T} \begin{bmatrix} \underline{\underline{\chi}}_b & 0 \\ 0 & \underline{\underline{\chi}}_b \end{bmatrix} \cdot \begin{bmatrix} \underline{\underline{V}} \\ \underline{\underline{i}} \end{bmatrix} + \begin{bmatrix} \underline{\underline{g}}_e * \underline{\underline{V}} \\ \underline{\underline{r}}_m * \underline{\underline{i}} \end{bmatrix} + \left(\frac{2\alpha_t}{\Delta\ell} \right) \frac{\partial}{\partial T} \begin{bmatrix} \underline{\underline{A}} & 0 \\ 0 & \underline{\underline{A}} \end{bmatrix} \cdot \begin{bmatrix} \underline{\underline{\chi}}_e & \underline{\underline{\xi}}_r \\ \underline{\underline{\zeta}}_r & \underline{\underline{\chi}}_m \end{bmatrix} \cdot \begin{bmatrix} \underline{\underline{\Delta}}^{-1} & 0 \\ 0 & \underline{\underline{\Delta}}^{-1} \end{bmatrix} * \begin{bmatrix} \underline{\underline{V}} \\ \underline{\underline{i}} \end{bmatrix}. \quad (11)$$

Approximating the normalized partial derivations in the curl matrix using the finite-differences of the voltages and currents on the surface of the TLM cell and applying the transformation to the travelling wave format as explained in [3], (11) can be written as:

$$\begin{aligned} & 2 \begin{bmatrix} V_0^i + V_1^i + V_2^i + V_3^i \\ V_4^i + V_5^i + V_6^i + V_7^i \\ V_8^i + V_9^i + V_{10}^i + V_{11}^i \\ -(V_6^i - V_7^i - V_8^i - V_9^i) \\ -(V_{10}^i - V_{11}^i - V_0^i - V_1^i) \\ -(V_2^i - V_3^i - V_4^i - V_5^i) \end{bmatrix} - \begin{bmatrix} i_{efx} \\ i_{efy} \\ i_{efz} \\ V_{mfx} \\ V_{mfy} \\ V_{mfz} \end{bmatrix} = \\ & = 4 \begin{bmatrix} \underline{\underline{V}} \\ \underline{\underline{i}} \end{bmatrix} + 2 \frac{\partial}{\partial T} \begin{bmatrix} \underline{\underline{\chi}}_b & 0 \\ 0 & \underline{\underline{\chi}}_b \end{bmatrix} \cdot \begin{bmatrix} \underline{\underline{V}} \\ \underline{\underline{i}} \end{bmatrix} + \begin{bmatrix} \underline{\underline{g}}_e * \underline{\underline{V}} \\ \underline{\underline{r}}_m * \underline{\underline{i}} \end{bmatrix} + \\ & + \left(\frac{2\alpha_t}{\Delta\ell} \right) \frac{\partial}{\partial T} \begin{bmatrix} \underline{\underline{A}} & 0 \\ 0 & \underline{\underline{A}} \end{bmatrix} \cdot \begin{bmatrix} \underline{\underline{\chi}}_e & \underline{\underline{\xi}}_r \\ \underline{\underline{\zeta}}_r & \underline{\underline{\chi}}_m \end{bmatrix} \cdot \begin{bmatrix} \underline{\underline{\Delta}}^{-1} & 0 \\ 0 & \underline{\underline{\Delta}}^{-1} \end{bmatrix} * \begin{bmatrix} \underline{\underline{V}} \\ \underline{\underline{i}} \end{bmatrix}. \quad (12) \end{aligned}$$

Defining the left-side of (12) as the excitation vector and introducing an effective susceptibility matrix as:

$$\begin{bmatrix} \underline{\underline{\chi}}_e^{eff} & \underline{\underline{\xi}}_r^{eff} \\ \underline{\underline{\zeta}}_r^{eff} & \underline{\underline{\chi}}_m^{eff} \end{bmatrix} = \begin{bmatrix} \underline{\underline{\chi}}_b & 0 \\ 0 & \underline{\underline{\chi}}_b \end{bmatrix} + \left(\frac{\alpha_t}{\Delta\ell} \right) \begin{bmatrix} \underline{\underline{A}} & 0 \\ 0 & \underline{\underline{A}} \end{bmatrix} \cdot \begin{bmatrix} \underline{\underline{\chi}}_e & \underline{\underline{\xi}}_r \\ \underline{\underline{\zeta}}_r & \underline{\underline{\chi}}_m \end{bmatrix} \cdot \begin{bmatrix} \underline{\underline{\Delta}}^{-1} & 0 \\ 0 & \underline{\underline{\Delta}}^{-1} \end{bmatrix}, \quad (13)$$

the final form of discrete-time solution of Maxwell's equations can be obtained as:

$$2 \begin{bmatrix} \underline{\underline{V}}^r \\ -\underline{\underline{i}}^r \end{bmatrix} = 4 \begin{bmatrix} \underline{\underline{V}} \\ \underline{\underline{i}} \end{bmatrix} + \begin{bmatrix} \underline{\underline{g}}_e * \underline{\underline{V}} \\ \underline{\underline{r}}_m * \underline{\underline{i}} \end{bmatrix} + 2 \frac{\partial}{\partial T} \begin{bmatrix} \underline{\underline{\chi}}_e^{eff} & \underline{\underline{\xi}}_r^{eff} \\ \underline{\underline{\zeta}}_r^{eff} & \underline{\underline{\chi}}_m^{eff} \end{bmatrix} * \begin{bmatrix} \underline{\underline{V}} \\ \underline{\underline{i}} \end{bmatrix}. \quad (14)$$

Previous expression can also be written as:

$$2 \underline{\underline{F}}^r = 4 \underline{\underline{F}} + \underline{\underline{\sigma}}(T) * \underline{\underline{F}} + 2 \frac{\partial}{\partial T} \left[\underline{\underline{M}}(T) * \underline{\underline{F}} \right], \quad (15)$$

where $\underline{\underline{\sigma}}(T)$ is conductivity matrix and $\underline{\underline{M}}(T)$ general material matrix, which also may contain some time dependent elements indicated explicitly with (T).

$$\underline{\underline{\sigma}}(T) = \begin{bmatrix} \underline{\underline{g}}_e & 0 \\ 0 & \underline{\underline{r}}_m \end{bmatrix}, \quad \underline{\underline{M}}(T) = \begin{bmatrix} \underline{\underline{\chi}}_e^{eff} & \underline{\underline{\xi}}_r^{eff} \\ \underline{\underline{\zeta}}_r^{eff} & \underline{\underline{\chi}}_m^{eff} \end{bmatrix}. \quad (16)$$

Using e.g., the bilinear Z-transform in the form $\partial / \partial T \approx 2(1-z^{-1}) / (1+z^{-1})$ (15) can be written as:

$$2(1+z^{-1}) \cdot \underline{\underline{F}}^r = (1+z^{-1}) \left(4 \underline{\underline{F}} + \underline{\underline{\sigma}}(z) \cdot \underline{\underline{F}} \right) + (1-z^{-1}) \underline{\underline{4M}}(z) \cdot \underline{\underline{F}}, \quad (17)$$

where z is a time shift operator. Additionally, matrix $\underline{\underline{4}} = 4\underline{\underline{1}}$.

In the modeling of matrices $\underline{\underline{\sigma}}(z)$ or $\underline{\underline{M}}(z)$ containing causal time-dependent elements, the overall strategy is to shift the time-dependence back to the previous time-step by taking partial fraction expansions as explained in [3,4]:

$$(1+z^{-1}) \underline{\underline{\sigma}}(z) = \underline{\underline{\sigma}}_0 + z^{-1} \left[\underline{\underline{\sigma}}_1 + \underline{\underline{\sigma}}_2(z) \right], \quad (18)$$

$$(1-z^{-1}) \underline{\underline{M}}(z) = \underline{\underline{M}}_0 - z^{-1} \left[\underline{\underline{M}}_1 + \underline{\underline{M}}_2(z) \right]. \quad (19)$$

III. COMPACT MODELING OF N-LAYER ANISOTROPIC MATERIAL

Proposed approach for a simulation of thin anisotropic multilayer material is based on acquiring the co-polarized and cross-polarized reflection and transmission coefficients in order to derivate the compact model. Hence, it is possible to eliminate the need to apply a fine mesh for modeling of material itself and replace it with interior boundary condition incorporated into a coarse mesh. When applying the compact model, the required number of cells and simulation run-time are significantly reduced in comparison with the fine mesh simulations.

The process of generating the compact model begins by numerically acquiring the co- and cross-polarized scattering parameters of thin anisotropic material by using the fine TLM mesh. Assuming that the thin anisotropic material is surrounded by air and placed in i -plane, the case of one-dimensional (1-D) propagation in i direction, with no coupling to the i -directed field components, has to be first considered. Two fine mesh time domain simulations have to be run with j - and k -polarized incident wave propagating in i direction, respectively. For each excitation, the incident field at the air-anisotropic material interface as well as the reflected and transmitted fields of appropriate polarization on both sides of this interface has to be recorded at each time-step so that the co-polarized and cross-polarized reflection and transmission coefficients of air-anisotropic material interface can be obtained using the following equations (20) and (21), respectively:

$$\begin{aligned} S_{11}^{kk} &= \frac{V_{reflected_field}^k}{V_{incident_field}^k}, S_{21}^{kk} = \frac{V_{transmitted_field}^k}{V_{incident_field}^k}, \\ S_{11}^{jj} &= \frac{V_{reflected_field}^j}{V_{incident_field}^j}, S_{21}^{jj} = \frac{V_{transmitted_field}^j}{V_{incident_field}^j}, \end{aligned} \quad (20)$$

$$S_{11}^{jk} = \frac{V_{reflected_field}^j}{V_{incident_field}^k}, S_{21}^{jk} = \frac{V_{transmitted_field}^j}{V_{incident_field}^k}, \quad (21)$$

$$S_{11}^{kj} = \frac{V_{reflected_field}^k}{V_{incident_field}^j}, S_{21}^{kj} = \frac{V_{transmitted_field}^k}{V_{incident_field}^j},$$

where index k is used to mark incident, reflected or transmitted field of k polarization and index j is used to mark incident, reflected or transmitted field of j polarization. The remaining co-polarized and cross-polarized reflection and transmission coefficients, S_{12} and S_{22} , can be found similarly considering j - and k -polarized incident wave propagating in $-i$ direction.

After performing the Fourier transform and translating parameters from time to frequency domain, the vector fitting (VF) method [16-18] is used to calculate rational approximations of n -th order (NP poles) of obtained co-polarized and cross-polarized reflection and transmission coefficients as:

$$S_{ij}^{pr} = \sum_{k=0}^{NP_{ij}^{pr}-1} C_{k,ij}^{pr} / (s - s_{pk,ij}^{pr}), \quad (22)$$

where $s_{pk,ij}^{pr}$ and $C_{k,ij}^{pr}$ are complex pole frequencies and residues, respectively, NP_{ij}^{pr} is a number of poles and $(ij) \in \{(11), (12), (21), (22)\}$, $(pr) \in \{(kk), (kj), (jk), (jj)\}$. Applying the bilinear Z-transform results in discrete-time representation of (22):

$$S_{ij}^{pr} = \frac{B_{0,ij}^{pr} + \sum_{k=1}^{NP_{ij}^{pr}} B_{k,ij}^{pr} z^{-k}}{1 + \sum_{k=1}^{NP_{ij}^{pr}} A_{k,ij}^{pr} z^{-k}} \xrightarrow{PFE} B_{0,ij}^{pr} \frac{\sum_{k=1}^{NP_{ij}^{pr}} B'_{k,ij} z^{-k}}{1 + \sum_{k=1}^{NP_{ij}^{pr}} A'_{k,ij} z^{-k}}, \quad (23)$$

where PFE stands for partial fraction expansion, $A'_{k,ij}$'s and $B'_{k,ij}$'s coefficients are real and the coefficients $B_{k,ij}^{pr} = B_{k,ij}^{pr} - B_{0,ij}^{pr} A_{k,ij}^{pr}$.

Digital filter-based compact model is then incorporated into the connection matrix of two TLM cells at which interface the anisotropic material is modeled as internal boundary condition (Fig. 1) so that:

$$\begin{bmatrix} V_k^{inc}[\bar{i}] \\ V_k^{inc}[\bar{i}+1] \end{bmatrix} = \begin{bmatrix} S_{11}^{kk} & S_{12}^{kk} \\ S_{21}^{kk} & S_{22}^{kk} \end{bmatrix} \begin{bmatrix} V_k^{ref}[\bar{i}] \\ V_k^{ref}[\bar{i}+1] \end{bmatrix} + \begin{bmatrix} S_{11}^{kj} & S_{12}^{kj} \\ S_{21}^{kj} & S_{22}^{kj} \end{bmatrix} \begin{bmatrix} V_j^{ref}[\bar{i}] \\ V_j^{ref}[\bar{i}+1] \end{bmatrix}, \quad (24)$$

$$\begin{bmatrix} V_j^{inc}[\bar{i}] \\ V_j^{inc}[\bar{i}+1] \end{bmatrix} = \begin{bmatrix} S_{11}^{jj} & S_{12}^{jj} \\ S_{21}^{jj} & S_{22}^{jj} \end{bmatrix} \begin{bmatrix} V_j^{ref}[\bar{i}] \\ V_j^{ref}[\bar{i}+1] \end{bmatrix} + \begin{bmatrix} S_{11}^{jk} & S_{12}^{jk} \\ S_{21}^{jk} & S_{22}^{jk} \end{bmatrix} \begin{bmatrix} V_k^{ref}[\bar{i}] \\ V_k^{ref}[\bar{i}+1] \end{bmatrix}, \quad (25)$$

where the incident and reflected voltage pulses orientations are defined with the respect of center of the TLM cells.

Considering that wave propagation can be observed along different axes of the Cartesian coordinate system, appropriate usage of TLM cell voltage pulses in (24) and

(25) for each direction accordingly is provided in Table 1.

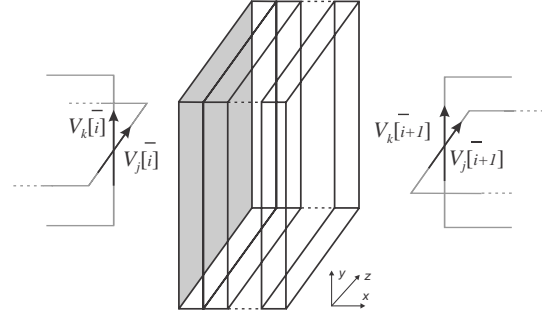


Fig. 1. Anisotropic n -layer material panel modeled as internal boundary condition.

Table 1: Voltage pulses notation based on wave propagation in i direction

i, j, k	$i \in x$	$i \in y$	$i \in z$
$V_k[\bar{i}]$	V_{12}	V_{10}	V_8
$V_k[\bar{i}+1]$	V_{11}	V_9	V_7
$V_j[\bar{i}]$	V_6	V_4	V_2
$V_j[\bar{i}+1]$	V_5	V_3	V_1

IV. MODELING RESULTS

The efficiency and accuracy of the compact modeling approach presented in section 3 is illustrated on two 2-D cases by using in-house developed TLM-Z code executed in MATLAB environment.

A. Symmetrical case

Thin single layered anisotropic material panel surrounded by air on both sides is placed in 2-D space (Fig. 2). Thickness of material is $d=1$ mm, isotropic relative permittivity has value of $\epsilon_r = 5$ while the electric conductivity is anisotropic and described with matrix:

$$\underline{\underline{\sigma}} = \begin{bmatrix} \sigma_{xx} & \sigma_{xy} & \sigma_{xz} \\ \sigma_{yx} & \sigma_{yy} & \sigma_{yz} \\ \sigma_{zx} & \sigma_{zy} & \sigma_{zz} \end{bmatrix}, \quad (26)$$

where $\sigma_{yy} = \sigma_{yz} = \sigma_{zy} = \sigma_{zz} = 100$ while the other matrix elements are equal to zero.

In order to obtain the co-polarized and cross-polarized reflection and transmission coefficients, as explained in section 3, an initial pulse of Gaussian form polarized first in z and then in y direction while propagating along the x axis was considered. 1-D Z-TLM fine mesh consisting out of 210 cells in x direction (10 cells to accurately represent EM field inside of the material) was used. Smallest dimension in model (in this case material panel) have to be described with minimum

5 cells and it is recommended to use at least 10 cells to represent minimum wavelength. Real and imaginary parts of co-polarized and cross-polarized reflection and transmission coefficients, obtained in such way are shown in Figs. 3 and 4. Due to symmetrical case,

$$S_{11}^{yy} = S_{22}^{yy} = S_{11}^{zz} = S_{22}^{zz}, S_{11}^{yz} = S_{22}^{yz} = S_{11}^{zy} = S_{22}^{zy},$$

$$S_{12}^{yy} = S_{21}^{yy} = S_{12}^{zz} = S_{21}^{zz} \text{ and } S_{12}^{yz} = S_{21}^{yz} = S_{12}^{zy} = S_{21}^{zy}.$$

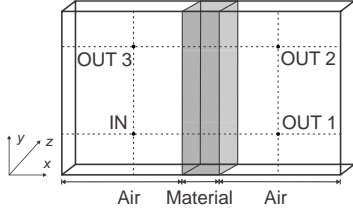


Fig. 2. Thin single layered anisotropic material placed in 2-D space.

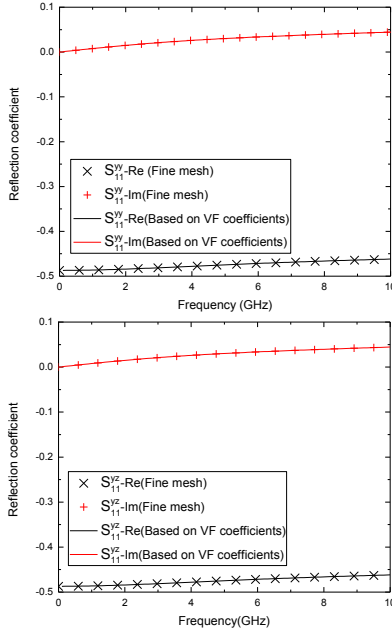


Fig. 3. Real and imaginary part of co-polarized and cross-polarized reflection coefficients (S_{11}^{yy} and S_{11}^{yz}) of thin single layered anisotropic material.

Next, coefficients A and B, obtained by the VF method in order to approximate the obtained reflection and transmission coefficients, are given in Table 2.

The rational approximations of 4-th order (number of poles $NP = 4$) is used to achieve needed accuracy. In [14] complex frequency dependence of reflection/transmission curves demanded rational approximations of 24th order. This neither influenced stability of method nor reduced accuracy of results but considering that higher number of poles increases computational time it

is recommended to find a proper balance. In some cases, reduction of frequency bandwidth in which the model is valid may reduce complexity of the approach and therefore can positively influence the modeling process. The approximated curves are shown also in Figs. 3 and 4.

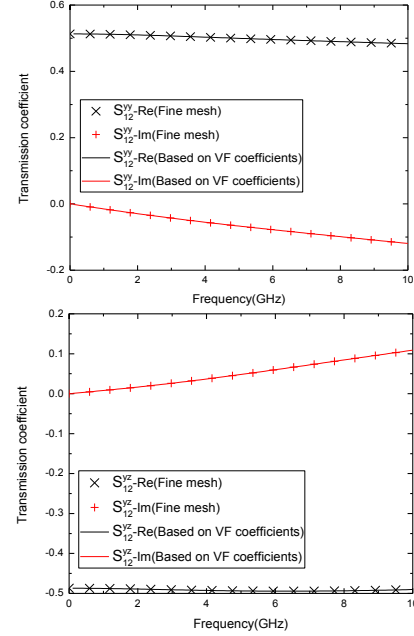


Fig. 4. Real and imaginary part of co-polarized and cross-polarized transmission coefficients (S_{12}^{yy} and S_{12}^{yz}) of thin single layered anisotropic material.

Thin single layered anisotropic material placed in 2-D space, as shown in Fig. 2, was considered in two ways:

- 1) Conventional approach by using the fine Z-TLM mesh to describe material (10 cells per thickness);
- 2) Proposed approach using coarse mesh and derived compact model placed at the position corresponding to the initial position of anisotropic material.

Fine mesh was consisted out of $882 \times 441 \times 1$ TLM cells. The number of time steps was 6300. Material is described with 10×441 cells while the rest of the cells are defined in areas filled with air. Excitation z-polarized source is placed at point marked as IN while electric field is observed in 3 different output points (OUT1, OUT2 and OUT3). Boundaries of the mesh in x and y planes are defined as absorbing while wrapped boundary conditions are used in z plane.

Compact model was incorporated into the coarse mesh with $42 \times 21 \times 1$ cells. Cell size is increased to $\Delta l = 2.1$ mm in order to preserve same modeling space. In that way, the number of cells is significantly reduced from 388962 cells, used in fine mesh, to only 882 cells (almost 99.78% less required cells) and the number of time steps is reduced from 6300 to 600.

Time-domain values of the electric field components in 3 output points, obtained by using the fine mesh (dotted lines) and course mesh with incorporated compact model (solid lines) are shown in Fig. 5. A good agreement between these two results can be observed.

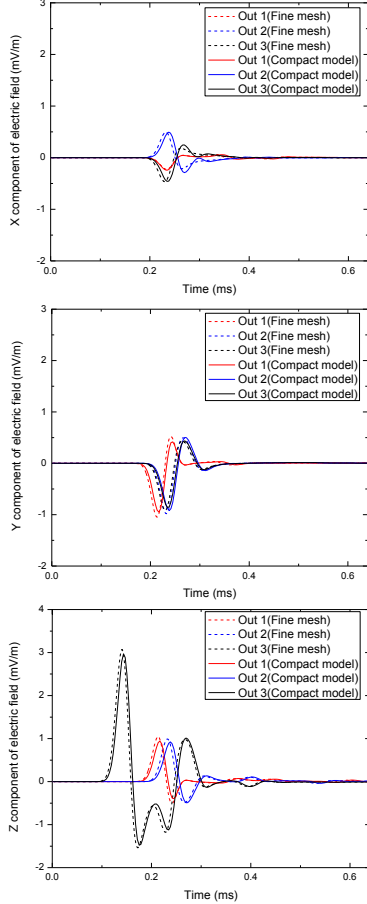


Fig. 5. Time-domain values of electric field components in 3 output points for thin single layered anisotropic material.

B. Asymmetrical case

In the second 2-D case, the composite general anisotropic material (Fig. 6) consists out of two layers of thickness $d_1=d_2=1$ mm, isotropic relative permittivity $\epsilon_r = 5$, and the anisotropic electric conductivities:

$$\underline{\underline{\sigma}}_1 = \begin{bmatrix} 0 & 0 & 0 \\ 0 & 100 & 100 \\ 0 & 100 & 100 \end{bmatrix}, \quad \underline{\underline{\sigma}}_2 = \begin{bmatrix} 0 & 0 & 0 \\ 0 & 100 & 0 \\ 0 & 0 & 500 \end{bmatrix}. \quad (27)$$

Overall dimensions and cell size of 1-D fine meshes, as well as 2-D fine mesh and 2-D coarse mesh with

incorporated compact model, are the same as in previously described single layered model. 10 cells per thickness are used for each layer.

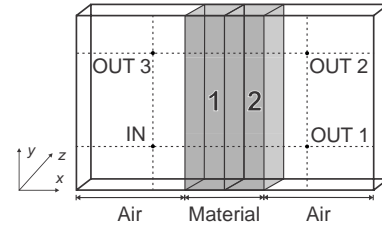


Fig. 6. Thin double layered anisotropic material placed in 2-D space.

Real and imaginary parts of some of co- and cross-polarization reflection and transmission coefficients of thin doubly layered anisotropic material are shown in Figs. 7-10.

Coefficients A and B, obtained by the VF method in order to approximate the obtained reflection and transmission coefficients, are given in Table 3. The approximated curves are shown also in Figs. 7-10.

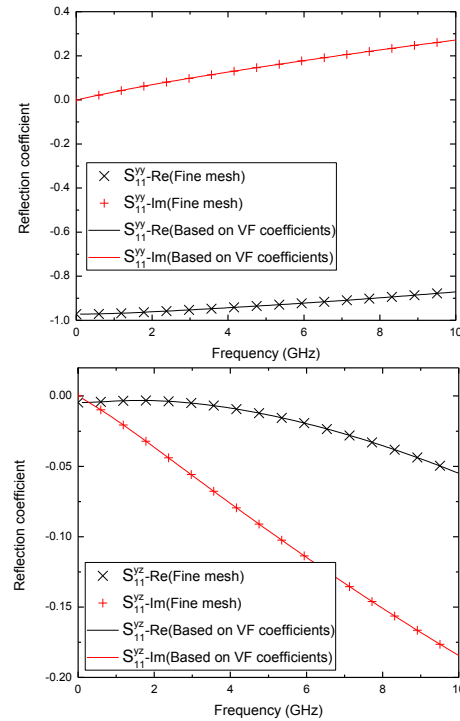


Fig. 7. Real and imaginary parts of co-polarized and cross-polarized reflection coefficients (S_{11}^{yy} and S_{11}^{yz}) of thin double layered anisotropic material.

Table 2: Coefficients used in (24) for compact representation of scattering parameters of single layered anisotropic material

Coefficient	$S_{11}^{yy} = S_{22}^{yy} = S_{11}^{zz} = S_{22}^{zz}$	$S_{11}^{yz} = S_{22}^{yz} = S_{11}^{zy} = S_{22}^{zy}$	$S_{12}^{yy} = S_{21}^{yy} = S_{12}^{zz} = S_{21}^{zz}$	$S_{12}^{yz} = S_{21}^{yz} = S_{12}^{zy} = S_{21}^{zy}$
B₀	-0.30415	-0.30415	0.063009	-0.06914
B_{prim}	-0.19535	-0.19534	0.271142	-0.24547
	0.454817	0.454811	-0.30291	0.099353
	-0.33921	-0.3392	-0.11521	0.07618
	0.079605	0.079601	0.150994	0.023792
A	1	1	1	1
	-2.02082	-2.02079	-1.94979	-1.40735
	0.942684	0.942647	1.278526	1.036736
	0.263883	0.263892	-0.48868	-0.65231
	-0.18501	-0.18501	0.168866	0.13335

Table 3: Coefficients used in (24) for compact representation of scattering parameters of double layered anisotropic material

Coefficient	S_{11}^{yy}	S_{11}^{zy}	S_{11}^{yz}	S_{11}^{zz}	S_{12}^{yy}	S_{12}^{zy}	S_{12}^{yz}	S_{12}^{zz}
B₀	-0.24811	-0.34991	-0.34991	-0.24751	-0.00064	-4.3E-05	0.000806	2.62E-05
B_{prim}	-0.36872	-0.05714	-0.05714	-0.36872	-0.00032	-5.1E-05	0.000567	3.32E-05
	0.938844	0.438528	0.438528	0.926638	0.002292	0.000184	-0.00276	-0.00011
	-0.8042	-0.68222	-0.68222	-0.77416	-0.00338	-0.00023	0.002462	0.000132
	0.232546	0.301308	0.301308	0.215514	0.001415	9.24E-05	-0.00028	-4.9E-05
A	1	1	1	1	1	1	1	1
	-3.03142	-2.0778	-2.0778	-3.00084	-3.36594	-3.5849	-2.69801	-3.51673
	3.418113	1.169718	1.169718	3.328296	4.257562	4.825226	2.615658	4.658698
	-1.69193	-0.03519	-0.03519	-1.61464	-2.40398	-2.89129	-1.06807	-2.75777
	0.30736	-0.05533	-0.05533	0.288149	0.512677	0.65106	0.152168	0.616004
Coefficient	S_{22}^{yy}	S_{22}^{zy}	S_{22}^{yz}	S_{22}^{zz}	S_{21}^{yy}	S_{21}^{zy}	S_{21}^{yz}	S_{21}^{zz}
B₀	-0.53567	9.19E-06	9.19E-06	-0.66253	-0.00064	0.000806	-4.3E-05	2.62E-05
B_{prim}	-0.40885	2.38E-05	2.38E-05	-0.39397	-0.00032	0.000567	-5.1E-05	3.32E-05
	1.018796	-5.4E-05	-5.4E-05	1.023097	0.002292	-0.00276	0.000184	-0.00011
	-0.83547	3.66E-05	3.66E-05	-0.8784	-0.00338	0.002462	-0.00023	0.000132
	0.224896	-6.4E-06	-6.4E-06	0.24896	0.001415	-0.00028	9.24E-05	-4.9E-05
A	1	1	1	1	1	1	1	1
	-2.29451	-3.62786	-3.62786	-2.21122	-3.36594	-2.69801	-3.5849	-3.51673
	1.48577	4.920007	4.920007	1.193826	4.257562	2.615658	4.825226	4.658698
	-0.02709	-2.95467	-2.95467	0.291451	-2.40398	-1.06807	-2.89129	-2.75777
	-0.16274	0.662553	0.662553	-0.2731	0.512677	0.152168	0.65106	0.616004

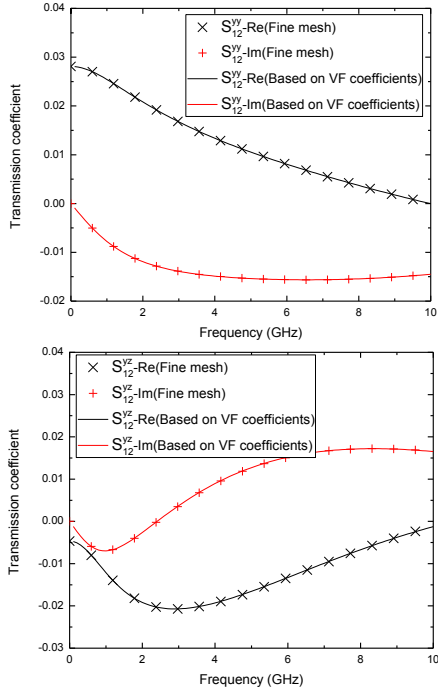


Fig. 8. Real and imaginary parts of co-polarized and cross-polarized transmission coefficients (S_{12}^{yy} and S_{12}^{yz}) of thin double layered anisotropic material.

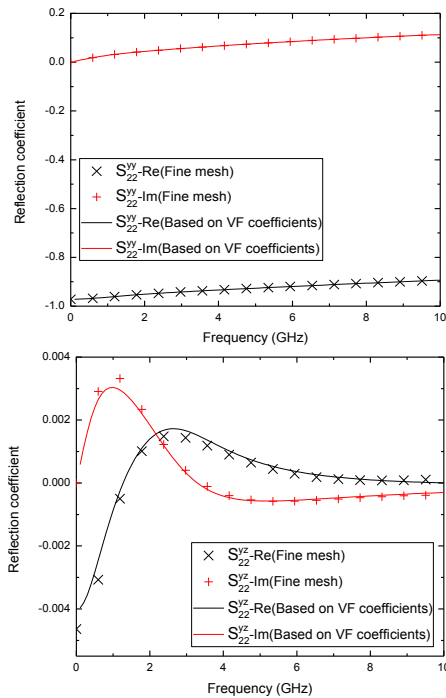


Fig. 9. Real and imaginary parts of co-polarized and cross-polarized reflection coefficients (S_{22}^{yy} and S_{22}^{yz}) of thin double layered anisotropic material.

Time-domain values of the electric field components in 3 output points, obtained by using the fine mesh (dotted lines) and course mesh with incorporated compact model (solid lines) are shown in Fig. 11. Results from point OUT3 for z component of electric field are shown separately for presentation purposes, because output values acquired in third point are much higher than results from first two points. A good agreement between these two results can be observed.

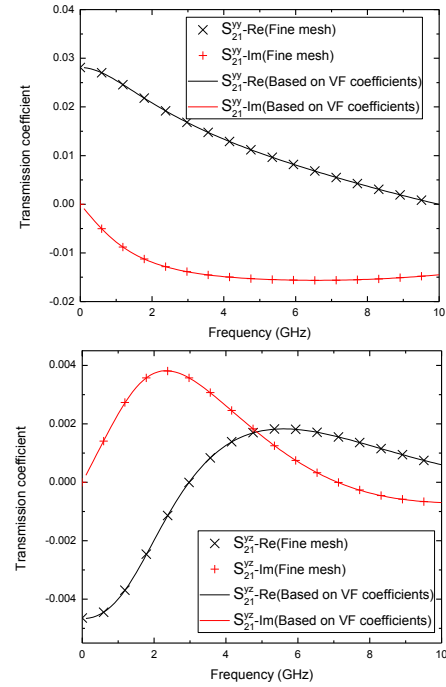
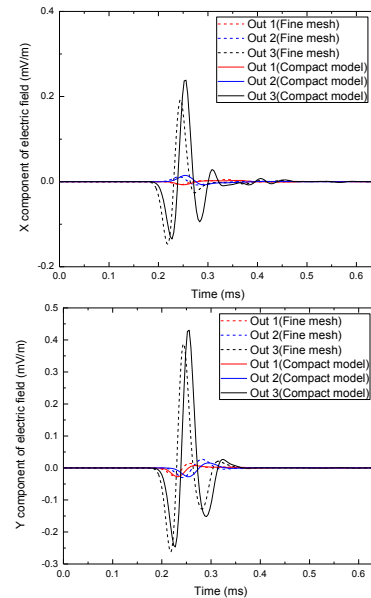


Fig. 10. Real and imaginary parts of co-polarized and cross-polarized transmission coefficients (S_{21}^{yy} and S_{21}^{yz}) of thin double layered anisotropic material.



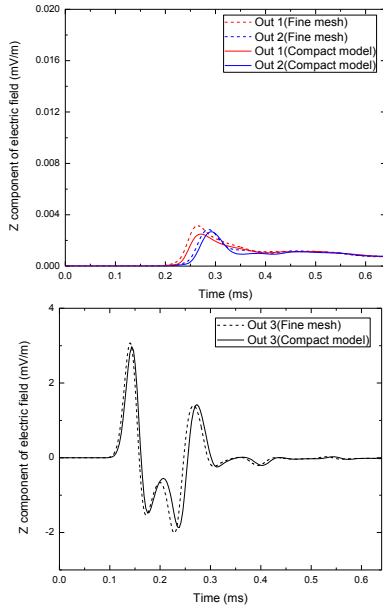


Fig. 11. Time-domain values of electric field components in 3 output points for thin double layered anisotropic material.

V. CONCLUSION

Efficient TLM based approach for compact modeling of anisotropic materials and composites is presented in this paper. Major advantage of this approach is significant reduction (over 99%) of mesh required for material modeling, which directly reduce computational costs and time. This can be very useful when modeling of thin multi-layered anisotropic material panels and structures. In future work, a proposed approach can be potentially applied for efficient modeling of anisotropic media in 3-D space.

ACKNOWLEDGMENT

This work has been supported by the Ministry of Education, Science and Technological Development of Serbia, project number TR32024.

REFERENCES

- [1] K. S. Kunz and R. J. Luebbers, *The Finite Difference Time Domain Method for Electromagnetics*. CRC Press, 1993.
- [2] C. Christopoulos, *The Transmission-Line Modelling (TLM) Method*. IEEE/OUP Press, 1995.
- [3] J. Paul, "Modelling of general electromagnetic material properties in TLM," *Ph.D. Dissertation*, University of Nottingham, UK, 1998.
- [4] J. Paul, C. Christopoulos, and D. W. P. Thomas, "Generalized material models in TLM – Part I: Materials with frequency-dependent properties," *IEEE Transactions on Antennas and Propagation*, vol. 47, no. 10, pp. 1528-1534, 1999.
- [5] J. Paul, C. Christopoulos, and D. W. P. Thomas, "Generalized material models in TLM – Part II: Materials with anisotropic properties," *IEEE Transactions on Antennas and Propagation*, vol. 47, no. 10, pp. 1535-1542, 1999.
- [6] J. Paul, C. Christopoulos, and D. W. P. Thomas, "Time-domain modelling of electromagnetic wave propagation in complex materials," *Electromagnetics*, vol. 19, no. 6, pp. 527-546, 1999.
- [7] J. Paul, C. Christopoulos, and D. W. P. Thomas, "Generalized material models in TLM – Part III: Materials with nonlinear properties," *IEEE Transactions on Antennas and Propagation*, vol. 50, no. 7, pp. 997-1004, 2002.
- [8] J. Paul, C. Christopoulos, and D. W. P. Thomas, "Time-domain simulation of electromagnetic wave propagation in two-level dielectrics," *International Journal of Numerical Modelling: Electronic Networks, Devices and Fields*, vol. 22, no. 2, pp. 129-141, 2009.
- [9] T. Asenov, N. Dončov, B. Milovanović, and J. Paul, "Dispersive TLM Z-transform model of left-handed metamaterials," *International Journal of Numerical Modelling: Electronic Networks, Devices and Fields*, vol. 26, no. 5, pp. 457-463, 2013.
- [10] J. Paul, V. Podlozny, D. W. P. Thomas, and C. Christopoulos, "Time-Domain simulation of thin material boundaries and thin panels using digital filters in TLM," *Turkish Journal of Electrical Engineering & Computer Sciences*, vol. 10, no. 2, pp. 185-198, 2002.
- [11] F. J. Hsieh and W. C. Wang, "Full extraction methods to retrieve effective refractive index and parameters of a bianisotropic metamaterial based on material dispersion models," *Journal of Applied Physics*, vol. 112, 064907, Sept. 2012.
- [12] P. Saguet, H. Louzani, and F. Ndagijimana, "The use of Z-transform in TLM with non-uniform meshes," *Proceedings of the Workshop on Computational Electromagnetics in Time-domain, CEM-TD 2005*, pp. 68-71, Atlanta, USA, 2005.
- [13] A. L. Farhat, S. L. Maguer, P. Queffelec, and M. Ney, "TLM extension to electromagnetic field analysis of anisotropic and dispersive media: A unified field equation," *IEEE Transactions on Microwave Theory and Techniques*, vol. 60, no. 8, pp. 2339-2351, 2012.
- [14] M. Kostić, N. Dončov, B. Stošić, and B. Milovanović, "Compact TLM model of dispersive anisotropic carbon-fibre material," *Proceedings of the 2nd International Conference on Electrical, Electronic and Computing Engineering, IcETRAN 2015*, Silver Lake, Serbia, pp. MT11.5.1-6, June 8-11, 2015.
- [15] V. Trenkic, A. P. Duffy, T. M. Benson, and C. Christopoulos, "Numerical simulation of

penetration and coupling using the TLM method," *EMC'94 Roma*, pp. 321-326, 13-16 Sept. 1994.

- [16] B. Gustavsen and A. Semlyen, "Rational approximation of frequency domain responses by vector fitting," *IEEE Trans. Power Delivery*, vol. 14, no. 3, pp. 1052-1061, July 1999.
- [17] B. Gustavsen, "Improving the pole relocating properties of vector fitting," *IEEE Trans. Power Delivery*, vol. 21, no. 3, pp. 1587-1592, July 2006.
- [18] D. Deschrijver, M. Mrozowski, T. Dhaene, and D. De Zutter, "Macromodeling of multiport systems using a fast implementation of the vector fitting method," *IEEE Microwave and Wireless Components Letters*, vol. 18, no. 6, pp. 383-385, June 2008.



Miloš Kostić received the Dipl.-Ing. degree from the Faculty of Electronic Engineering, University of Nis, Serbia, in 2013. Currently he works as Junior Researcher at Innovation Center of Advanced Technologies (ICAT), Serbia. His research interests are numerical modeling of isotropic and anisotropic materials and meta materials and their application in microwave structures.



Nebojša Dončov received the Dipl.-Ing., M.Sc., and Ph.D. degrees from the Faculty of Electronic Engineering, University of Nis, Serbia, in 1995, 1999 and 2002, respectively. Currently, he is a Full Professor at the Faculty of Electronic Engineering, Serbia. His research interests are in computational and applied electromagnetics with a particular emphasis on TLM and neural networks applications in microwaves and EMC. Dončov was the recipient of the International Union of Radio Science (URSI) Young Scientist Award in 2002.

Zoran Stanković received the Dipl.-Ing., M.Sc., and Ph.D. degrees from the Faculty of Electronic Engineering, University of Nis, Serbia, in 1994, 2002 and 2007, respectively. Currently, he is an Assistant Professor at the Department of Telecommunications, Faculty of Electronic Engineering, Serbia. His research interests include neural networks applications in the field of electromagnetics, wireless communications systems and computer communications. Stanković was the recipient of the National MTT Society Award in 2005 for the outstanding scientific results in the area of microwave techniques.



John Paul received the M.Eng. and the Ph.D. degrees in Electrical and Electronic Engineering from the University of Nottingham, U.K., in 1994 and 1999, respectively. His Ph.D. thesis involved the application of signal processing and control system techniques to the simulation of general material properties in time-domain TLM. He was employed as a Senior Research Fellow with the George Green Institute for Electromagnetics Research at the University of Nottingham, U.K. His research interests are in the application of signal processing techniques for advanced material modeling in time-domain computational electromagnetics and the simulation of complete systems for electromagnetic compatibility studies.